

## Supporting information

# Facilely Tunable Redox Behaviors in Donor-node-Acceptor Polymers toward High-Performance Ambipolar Electrode Materials

*Hailong Wang, Nianqiang Jiang, Qinglei Zhang, Guojing Xie, Ningning Tang, Linlin Liu, Zengqi Xie\**

State Key Laboratory of Luminescent Materials and Devices, South China University of Technology, Institute of Polymer Optoelectronic Materials and Devices, Guangdong Provincial Key Laboratory of Luminescence from Molecular Aggregates, Guangzhou 510640, P. R. China

### Table of contents

1. Experimental Section .....	S2
2. Specific Capacitances .....	S2
3. Synthesis and Characterization .....	S3
4. Single crystal structure of 4T-PDI and 2T <sub>3</sub> -PDI .....	S11
5. DFT Theoretical Calculation.....	S12
6. Electrochemical Properties of the Monomer.....	S13
7. Electrochemical Synthesis and Characterization of the Polymer Films.....	S14
8. Capacitance of poly-2T <sub>3</sub> -PDI with literature .....	S25
8. Reference .....	S27

## 1. Experimental Section

**Materials and Methods.** Solvents and reagents were purchased from commercial sources and were used as received, unless otherwise stated. Column chromatography was performed with silica gel (Hai Yang Silica 60, particle size 0.035-0.070 mm).  $^1\text{H}$  and  $^{13}\text{C}$  NMR were recorded using a Bruker-300 spectrometer operating at 500 and 75 MHz in deuterated chloroform and dichloroethane solution at 298 K. Chemical shifts were reported as  $\delta$  values (ppm) relative to an internal tetramethylsilane (TMS) standard. The UV-vis absorption and fluorescence spectra were recorded on a Shimadzu UV-3600 and spectro-photometer, respectively. Cyclic voltammetry (CV), galvanostatic charge/discharge and EIS with frequency ranging from 0.1 Hz to 100 kHz measurement was performed on a CHI760E electrochemical workstation.

**Electrochemical Polymerization of Polymer Network Film.** The  $\text{Ag}/\text{Ag}^+$  electrode with  $\text{AgNO}_3$  (0.01 M) in acetonitrile was used as reference electrode. The monomer (0.015 M) was dissolved in the  $\text{CH}_2\text{Cl}_2$  together with  $\text{Bu}_4\text{NPF}_6$  (0.1 M) as the supporting electrolyte. ITO was used as the working electrode and titanium metal was used as the counter electrode. The scanning rate was  $100 \text{ mV s}^{-1}$ . The polymer film obtained by electrochemical polymerization were dried for 8 hours at  $40^\circ\text{C}$  in a vacuum oven, and then the thickness was measured by Veeco dektak 150 Level gauge instrument. The relationship between the thickness and number of cycles plots were studied through independent samples with different number of cycles.

The electrode mass is weighed using a Mettler Toledo XP6 ultramicrobalance with an accuracy of 0.001 mg.

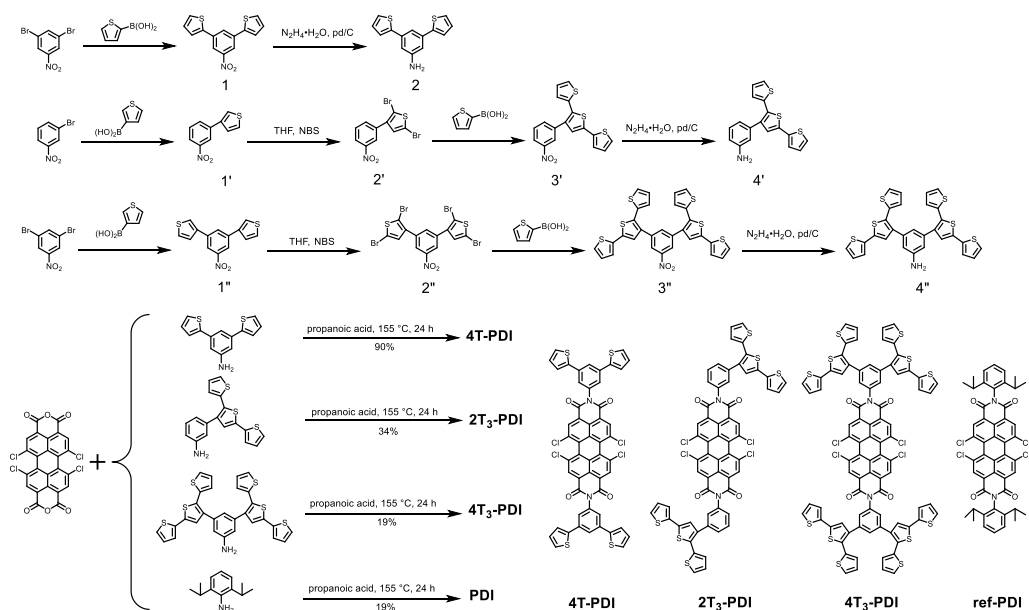
### Specific Capacitances

The **specific capacitances** (C) from the galvanostatic charge/discharge curves in three-electrode configuration were calculated using Equation (1):

$$C = \frac{I\Delta t}{m\Delta V} \quad (1)$$

in which  $I$  is the discharge current,  $\Delta t$  is the discharge time,  $m$  is the mass of the active electrode material and  $\Delta V$  is the potential window.

## 2. Synthesis and Characterization



Scheme S1. Synthetic routes of 4T-PDI, 2T<sub>3</sub>-PDI, 4T<sub>3</sub>-PDI and ref-PDI.

### Synthesis of 4T-PDI:

#### Synthesis of Compound 1:

A mixture of 3,5-dibromonitrobenzene (1.0 g, 3.6 mmol), 2-thiopheneboronic acid (1.4 g, 10.8 mmol), dioxane (35 ml), aqueous sodium carbonate (Na<sub>2</sub>CO<sub>3</sub>) (2 mol/L, 9 mL) and tetrakis(triphenylphosphine)palladium (415 mg, 0.36 mmol) was heated at 85 °C for 12 h under argon. After cooling to room temperature, the mixture was quenched with distilled water, and then the precipitate was extracted with ethyl acetate

(EA). After evaporation of the solvent, the crude product was purified by column chromatography eluting with mixed solvent (petroleum ether (PE): EA = 2:1) to give a yellow solid (1.0 g). Yield: 98%.  $^1\text{H}$  NMR (400 MHz,  $\text{CDCl}_3$ )  $\delta$  8.33 (d,  $J$  = 1.7 Hz, 2H), 8.07 (t,  $J$  = 1.7 Hz, 1H), 7.48 (dd,  $J$  = 3.6, 1.2 Hz, 2H), 7.41 (dd,  $J$  = 5.1, 1.1 Hz, 2H), 7.16 (dd,  $J$  = 5.1, 3.6 Hz, 2H).

#### Synthesis of Compound 2:

A mixture of the compound 1 (1.0 g, 3.5 mmol), 10% pd/c (1.2 g), ethanol (40 ml), 80% hydrazine hydrate (1.2 ml) was heated at 85 °C for 12 h under argon. The mixture is filtered, and the filtrate concentrated under pressure to leave a crude residue. The crude product was purified by washing with water five times to provide the compound 5 as a white solid (0.87 g). Yield: 98%.  $^1\text{H}$  NMR (400 MHz,  $\text{CDCl}_3$ )  $\delta$  7.32 (dd,  $J$  = 3.6, 1.2 Hz, 2H), 7.29 (d,  $J$  = 1.2 Hz, 1H), 7.28-7.26 (m, 2H), 7.08 (dd,  $J$  = 5.1, 3.6 Hz, 2H), 6.86 (d,  $J$  = 1.6 Hz, 2H), 3.79 (s, 2H)

#### Synthesis of 4T-PDI:

A mixture of compound 2 (0.82 g, 3.2 mmol), tetrachlorinated 3, 4,9, 10-perylenetetracarboxylic dianhydride (530 mg, 1.0 mmol), and 15 ml propionic acid was heated at 150 °C for 24 h. After cooling to room temperature, the mixture was washed with water and methanol, dried in a vacuum oven. the crude product was purified by column chromatography eluting with mixed solvent (PE : DCM = 1:2) to give a fluffy red solid (906 mg). Yield: 90 %.  $^1\text{H}$  NMR (400 MHz,  $\text{CDCl}_3$ )  $\delta$  8.78 (s, 4H), 7.97 (t,  $J$  = 1.6 Hz, 2H), 7.47 (d,  $J$  = 1.6 Hz, 4H), 7.41 (dd,  $J$  = 3.7, 1.2 Hz, 4H), 7.35 (dd,  $J$  =

5.0, 1.1 Hz, 4H), 7.12 (dd,  $J = 5.1, 3.6$  Hz, 4H).  $^{13}\text{C}$  NMR (101 MHz,  $\text{CDCl}_3$ )  $\delta$  162.32, 142.74, 136.71, 135.72, 133.42, 129.03, 128.17, 125.80, 124.94, 124.29, 123.36 ppm; MALDI-TOF (m/s): calcd. for  $\text{C}_{52}\text{H}_{22}\text{Cl}_4\text{N}_2\text{O}_4\text{S}_4$  1007.9187; found, 1007.8983. The single crystal structure of 4T-PDI (cif) was deposited in the Cambridge database (CCDC 2058754).

### Synthesis of 2T<sub>3</sub>-PDI:

#### Synthesis of Compound 1':

A mixture of 3-dibromonitrobenzene (1.5 g, 7.4 mmol), 3-thiopheneboronic acid (1.42 g, 11.1 mmol), dioxane (35 ml), aqueous sodium carbonate ( $\text{Na}_2\text{CO}_3$ ) (2 mol/L, 12 mL) and tetrakis(triphenylphosphine) palladium (427 mg, 0.37 mmol) was heated at 85 °C for 12 h under argon. After cooling to room temperature, the mixture was quenched with distilled water, and then the precipitate was extracted with ethyl acetate (EA). After evaporation of the solvent, the crude product was purified by column chromatography eluting with mixed solvent (petroleum ether (PE): EA = 2:1) to give a white yellow solid (1.49 g). Yield: 98%.  $^1\text{H}$  NMR (400 MHz,  $\text{CDCl}_3$ )  $\delta$  8.44 (t,  $J = 1.9$  Hz, 1H), 8.14 (ddd,  $J = 8.2, 2.2, 1.0$  Hz, 1H), 7.91 (ddd,  $J = 7.8, 1.7, 1.0$  Hz, 1H), 7.58 (dt,  $J = 16.2, 4.7$  Hz, 2H), 7.45 (qd,  $J = 5.0, 2.2$  Hz, 2H).

#### Synthesis of Compound 2':

The reaction of the compound 1' (1.4 g, 6.8 mmol), N-bromosuccinimide (NBS) (3.72 g, 20.4 mmol) and 50 ml Tetrahydrofuran (THF) at 0 °C for 1 hours under nitrogen.

After 1 hours, the reaction was carried out at room temperature for 48 h. After evaporation of the mixture, the crude product was purified by column chromatography eluting with mixed solvent (PE:EA = 15:1) to give a fluffy dark brown solid (2.44 g). Yield: 99%.  $^1\text{H}$  NMR (400 MHz,  $\text{CDCl}_3$ )  $\delta$  8.38 (t,  $J$  = 1.9 Hz, 1H), 8.23 (dd,  $J$  = 8.2, 1.7 Hz, 1H), 7.84 (d,  $J$  = 7.7 Hz, 1H), 7.62 (t,  $J$  = 8.0 Hz, 1H), 7.07 (s, 1H).

#### Synthesis of Compound 3':

A mixture of the compound 2' (2 g, 5.5 mmol), 2-thiopheneboronic acid (2.1 g, 16.5 mmol), dioxane (50 ml), aqueous  $\text{Na}_2\text{CO}_3$  (2 mol/L, 14 mL) tetrakis(triphenylphosphine) palladium (317 mg, 0.27 mmol), was heated at 85 °C for 12 h under argon. After cooling to room temperature, the mixture was quenched with distilled water, and then the precipitate was extracted with EA. After evaporation of the solvent, the crude product was purified by column chromatography eluting with mixed solvent (PE:EA = 2:1) to give a fluffy yellow solid (1.99 g). Yield: 98%.  $^1\text{H}$  NMR (400 MHz,  $\text{CDCl}_3$ )  $\delta$  8.20 (t,  $J$  = 1.9 Hz, 1H), 8.10 (ddd,  $J$  = 8.2, 2.3, 1.0 Hz, 1H), 7.64-7.59 (m, 1H), 7.43 (dd,  $J$  = 9.8, 6.1 Hz, 1H), 7.19 (dt,  $J$  = 4.8, 2.0 Hz, 1H), 7.17-7.13 (m, 2H), 7.09 (s, 1H), 6.97 (dd,  $J$  = 5.1, 3.6 Hz, 1H), 6.93-6.86 (m, 2H).

#### Synthesis of Compound 4':

A mixture of the compound 3' (1.5 g, 4.1 mmol), 10% Pd/C (1.5 g), ethanol (60 ml), 80% hydrazine hydrate (1.5 ml) was heated at 85 °C for 12 h under argon. The mixture is filtered, and the filtrate concentrated under pressure to leave a crude residue. The crude product was purified by washing with water five times to provide the compound 5 as a

white yellow solid (1.36 g). Yield: 98%.  $^1\text{H}$  NMR (400 MHz,  $\text{CDCl}_3$ )  $\delta$  7.15 (dd,  $J$  = 5.1, 1.1 Hz, 1H), 7.13-7.03 (m, 4H), 6.97-6.93 (m, 2H), 6.85 (dd,  $J$  = 5.1, 3.6 Hz, 1H), 6.72-6.68 (m, 1H), 6.65-6.57 (m, 2H), 3.59 (s, 2H).

#### Synthesis of 2T<sub>3</sub>-PDI:

A mixture of compound 4" (1 g, 2.9 mmol), tetrachlorinated 3, 4,9, 10-perylenetetracarboxylic dianhydride (512 mg, 0.96 mmol), and 10 ml propionic acid was heated at 150 °C for 24 h. After cooling to room temperature, the mixture was washed with water and methanol, dried in a vacuum oven. the crude product was purified by column chromatography eluting with mixed solvent (PE:DCM = 1:3) to give a fluffy yellow solid (356 mg). Yield: 31.6 %.  $^1\text{H}$  NMR (500 MHz,  $\text{C}_2\text{D}_2\text{Cl}_4$ )  $\delta$  8.76 (s, 1H), 7.67 (dt,  $J$  = 15.2, 7.7 Hz, 1H), 7.46 (s, 1H), 7.38 (d,  $J$  = 7.7 Hz, 1H), 7.35-7.26 (m, 2H), 7.16-7.09 (m, 1H), 7.08-7.00 (m, 1H).  $^{13}\text{C}$  NMR (126 MHz,  $\text{C}_2\text{D}_2\text{Cl}_4$ )  $\delta$  162.47, 137.81, 137.49, 136.61, 135.74, 135.68, 135.19, 134.81, 133.37, 131.68, 131.21, 130.21, 129.93, 129.49, 129.00, 128.29, 127.93, 127.81, 126.99, 126.95, 126.35, 125.21, 124.27, 123.74, 123.40 ppm; MALDI-TOF (m/s): calcd. for  $\text{C}_{60}\text{H}_{26}\text{Cl}_4\text{N}_2\text{O}_4\text{S}_6$  1171.8941; found, 1171.8835. The single crystal structure of 2T<sub>3</sub>-PDI (cif) was deposited in the Cambridge database (CCDC 2058754).

#### Synthesis of 4T<sub>3</sub>-PDI:

#### Synthesis of Compound 1":

A mixture of 3,5-dibromonitrobenzene (2.0 g, 7.1 mmol), 3-Thiopheneboronic acid (2.73 g, 21.3 mmol), dioxane (60 ml), aqueous sodium carbonate (2 mol/L, 18 mL), and Tetrakis(triphenylphosphine) palladium (820 mg, 0.71 mmol) was heated at 85 °C for 12 h under argon. After cooling to room temperature, the mixture was quenched with distilled water, and then the precipitate was extracted with ethyl acetate (EA). After evaporation of the solvent, the crude product was purified by column chromatography eluting with mixed solvent (petroleum ether (PE):EA = 2:1) to give a fluffy white yellow solid (2.0 g). Yield: 98%. <sup>1</sup>H NMR (400 MHz, CDCl<sub>3</sub>) δ 8.37 (d, *J* = 1.6 Hz, 2H), 8.12 (t, *J* = 1.6 Hz, 1H), 7.66 (dd, *J* = 2.8, 1.6 Hz, 2H), 7.52-7.48 (m, 4H).

#### Synthesis of Compound 2":

The reaction of the compound 1" (1.8 g, 6.3 mmol), N-bromosuccinimide (NBS) (6.73 g, 37.8 mmol) and 100 ml THF at 0 °C for 1 hours under nitrogen. After 1 hours, the reaction was carried out at room temperature for 48 h. After evaporation of the mixture, the crude product was purified by column chromatography eluting with mixed solvent (PE:EA = 15:1) to give a dark brown solid (3.75 g). Yield: 99%. <sup>1</sup>H NMR (400 MHz, CDCl<sub>3</sub>) δ 8.38 (d, *J* = 1.6 Hz, 2H), 7.97 (t, *J* = 1.6 Hz, 1H), 7.11 (d, *J* = 3.9 Hz, 2H).

#### Synthesis of Compound 3":

A mixture of the compound 2" (3.0 g, 5.0 mmol), 2-thiopheneboronic acid (3.84 g, 30 mmol), dioxane (80 ml), aqueous sodium carbonate (2 mol/L, 25 mL), and



tetrakis(triphenylphosphine)palladium (577 mg, 0.5 mmol) was heated at 85 °C for 12 h under argon. After cooling to room temperature, the mixture was quenched with distilled water, and then the precipitate was extracted with EA. After evaporation of the solvent, the crude product was purified by column chromatography eluting with mixed solvent (PE: EA = 2:1) to give a fluffy yellow solid (2.9 g). Yield: 95%. <sup>1</sup>H NMR (400 MHz, CDCl<sub>3</sub>): δ 8.19 (d, J = 1.5 Hz, 2H), 7.71 (t, J = 1.5 Hz, 1H), 7.29-7.27 (m, 4H), 7.22 (dd, J = 3.6, 1.0 Hz, 2H), 7.09-6.99 (m, 8H).

#### Synthesis of Compound 4":

A mixture of the compound 3" (2.4 g, 3.9 mmol), 10% pd/c (2.5 g), ethanol (70 ml), and 80% hydrazine hydrate (2.6 ml) was heated at 85 °C for 12 h under argon. The mixture is filtered, and the filtrate concentrated under pressure to leave a crude residue. The crude product was purified by washing with water five times to provide the compound 5 as a white yellow solid (2.05 g). Yield: 90%. <sup>1</sup>H NMR (500 MHz, C<sub>2</sub>D<sub>2</sub>Cl<sub>4</sub>) δ 7.29-7.20 (m, 6H), 7.11-7.04 (m, 6H), 6.98 (dt, J = 8.9, 4.4 Hz, 2H), 6.83 (t, J = 1.3 Hz, 1H), 6.69 (dd, J = 10.1, 1.7 Hz, 2H), 3.74 (s, 2H).

#### Synthesis of 4T<sub>3</sub>-PDI:

A mixture of compound 4" (1.8 g, 3.1 mmol), tetrachlorinated 3, 4,9, 10-perylenetetracarboxylic dianhydride (530 mg, 1.0 mmol), and 10 ml propionic acid was heated at 150 °C for 24 h. After cooling to room temperature, the mixture was washed with water and methanol, dried in a vacuum oven. the crude product was purified by column chromatography eluting with mixed solvent (PE : DCM = 1:3) to

give a fluffy yellow solid (349 mg). Yield: 21%.  $^1\text{H}$  NMR (500 MHz,  $\text{C}_2\text{D}_2\text{Cl}_4$ )  $\delta$  8.70 (s, 4H), 7.59 (t,  $J = 1.5$  Hz, 2H), 7.38 (d,  $J = 1.5$  Hz, 4H), 7.30 (ddd,  $J = 12.4, 5.1, 1.0$  Hz, 8H), 7.22 (dd,  $J = 3.5, 1.0$  Hz, 4H), 7.18 (s, 4H), 7.13 (dd,  $J = 3.6, 1.1$  Hz, 4H), 7.05 (ddd,  $J = 14.1, 5.1, 3.6$  Hz, 8H).  $^{13}\text{C}$  NMR (126 MHz,  $\text{C}_2\text{D}_2\text{Cl}_4$ )  $\delta$  162.32, 162.30, 137.57, 137.50, 137.48, 136.61, 136.59, 135.81, 135.69, 135.10, 135.08, 133.32, 131.66, 131.21, 128.96, 128.63, 128.27, 128.24, 127.86, 127.84, 127.18, 126.79, 126.51, 126.48, 125.22, 124.26, 124.23, 123.71, 123.41 ppm; MALDI-TOF (m/s): calcd. for  $\text{C}_{84}\text{H}_{38}\text{Cl}_4\text{N}_2\text{O}_4\text{S}_{12}$  1165.8205; found, 1165.8243.

### Synthesis of ref-PDI:

A mixture of 2,6-diisopropylaniline (2.0 g, 11.3 mmol), tetrachlorinated 3,4,9,10-perylenetetracarboxylic dianhydride (2.4 g, 4.52 mmol), and 10 ml propionic acid was heated at 150 °C for 24 h. After cooling to room temperature, the mixture was washed with water and methanol, dried in a vacuum oven. the crude product was purified by column chromatography eluting with mixed solvent (PE: DCM = 1:1) to give a fluffy yellow solid (3.75 g). Yield: 95%.  $^1\text{H}$  NMR (400 MHz, Chloroform- $d$ )  $\delta$  8.79 (s, 4H), 7.54 (t,  $J = 7.8$  Hz, 2H), 7.38 (d,  $J = 7.8$  Hz, 4H), 2.83-2.68 (m, 4H), 1.24-1.13 (m, 24H).  $^{13}\text{C}$  NMR (101 MHz,  $\text{CDCl}_3$ )  $\delta$  162.37 (s), 145.63 (s), 135.68 (s), 133.49 (s), 131.78 (s), 129.98 (d,  $J = 18.7$  Hz), 128.96 (s), 124.31 (s), 123.97 (s), 123.25 (s), 29.32 (s), 24.06 (s). MALDI-TOF (m/s): calcd. for  $\text{C}_{52}\text{H}_{22}\text{Cl}_4\text{N}_2\text{O}_4$  848.6383; found, 848.6354.

### 3. Single crystal structure of 4T-PDI and 2T<sub>3</sub>-PDI

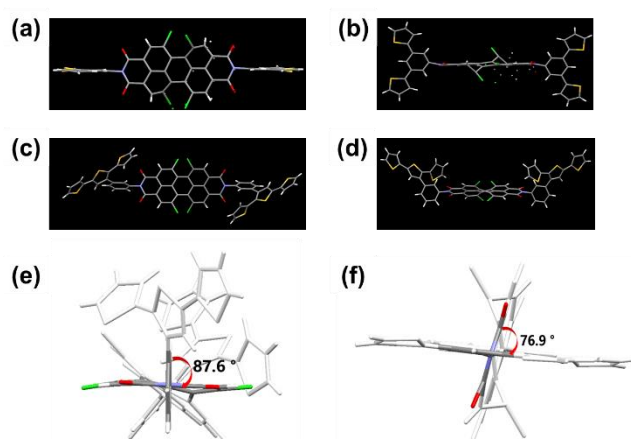


Figure S1. Top view of the molecules in single crystal: (a) 4T-PDI, (c) 2T<sub>3</sub>-PDI; side view of molecules in single crystal: (b) 4T-PDI, (d) 2T<sub>3</sub>-PDI; the angle between the phenyl group and the O=C-N-C=O imide group plane: (e) 2T<sub>3</sub>-PDI, (f) 4T-PDI.

The single crystals of 4T-PDI and 2T<sub>3</sub>-PDI were successfully obtained by liquid diffusion method, and the single crystal X-ray diffraction data were then collected for crystal structure analysis. Figure S1a-d showed the molecular conformation in the single crystal structure. The single crystal structure of 4T-PDI (Figure S1e) and 2T<sub>3</sub>-PDI (Figure S1f) showed that the phenyl group and the O=C-N-C=O imide group plane form angles of 76.9 and 87.6 degrees, respectively, which are closer to 90 degrees.

#### 4. DFT Theoretical Calculation

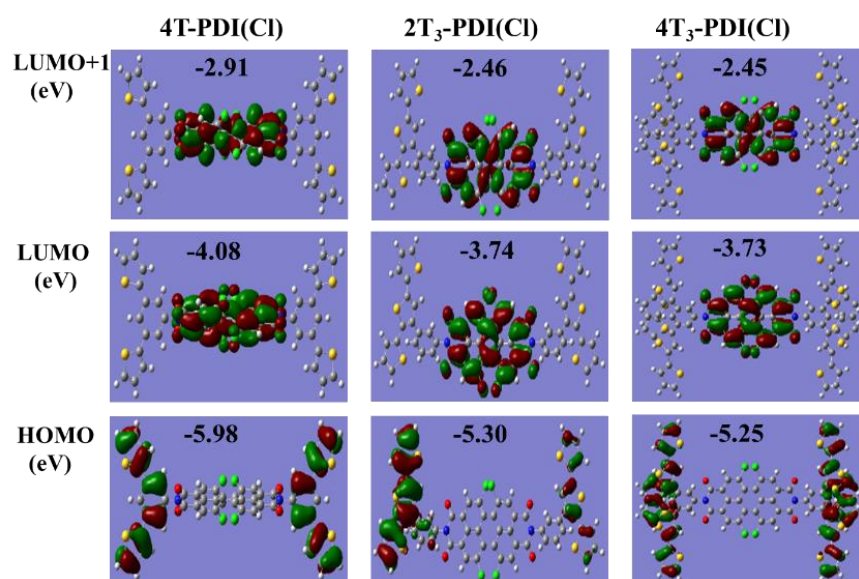


Figure S2. Selected frontier molecular orbitals and energy levels of monomer 4T-PDI, 2T<sub>3</sub>-PDI and 4T<sub>3</sub>-PDI calculated by DFT (B3LYP/6-31G (d)).

The energy levels of the orbits are presented in shown [Figure S2](#). For all three compounds, the lowest unoccupied molecular orbital (LUMO) orbital is distributed on the PDI moiety (acceptor moiety). Furthermore, The LUMO+1 orbital of 4T-PDI, 2T<sub>3</sub>-PDI and 4T<sub>3</sub>-PDI are all completely confined on the perylene cores. The result indicated that the perylene cores can store two electrons to form anion and dianion. The highest occupied molecular orbital (HOMO) is confined on the benzene-thiophene moiety (donor moiety). The HOMO (or LUMO) value for 4T-PDI was about 0.84 V (or 0.35 V) lower than that of 2T<sub>3</sub>-PDI and 4T<sub>3</sub>-PDI, which might be caused by the difference in the number and connection mode of thiophene units. As can be calculated, the LUMO and LUMO+1 exhibits no overlapping with HOMO, suggesting that the two N-

nodes break the conjugation between donor and acceptor units. This result indicated that the three D-n-A molecules can independently undergo redox activity.

## 5. Electrochemical Properties of the Monomer

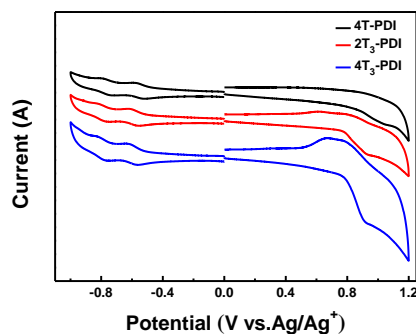


Figure S3. Cyclic voltammograms of the monomer molecules ( $5 \times 10^{-5}$  mol L<sup>-1</sup>) recorded using glassy carbon as the working electrode, Bu<sub>4</sub>NPF<sub>6</sub> as supporting electrolyte (0.1 mol L<sup>-1</sup>), scan rate of 100 mV s<sup>-1</sup>.

Table S1. Electrochemical properties of the three monomers calculated from cyclic voltammetry.

PDI <sub>s</sub>	E <sub>red onset</sub> <sup>a</sup> (V)	LUMO <sup>b</sup> (eV)	E <sub>ox onset</sub> <sup>a</sup> (V)	HOMO <sup>c</sup> (eV)	LUMO-HOMO (eV)
4T-PDI	-0.70	-4.10	0.61	-5.41	1.31
2T <sub>3</sub> -PDI	-0.74	-4.06	0.54	-5.34	1.28
4T <sub>3</sub> -PDI	-0.74	-4.06	0.56	-5.36	1.28

<sup>a</sup> 0.1 M Bu<sub>4</sub>NPF<sub>6</sub> in DCM vs. Ag/Ag<sup>+</sup>; <sup>b</sup> Estimated LUMO level from eqn E<sub>LUMO</sub> (eV) = - (E<sub>red onset</sub> + 4.8) = - (E<sub>pc onset</sub> - E<sub>Fc</sub> + 4.8 eV); <sup>c</sup> Estimated HOMO level from eqn E<sub>HOMO</sub> (eV) = - (E<sub>ox onset</sub> + 4.8) = - (E<sub>pc onset</sub> - E<sub>Fc</sub> + 4.8 eV).<sup>1-3</sup>

The electrochemical properties of 4T-PDI, 2T<sub>3</sub>-PDI and 4T<sub>3</sub>-PDI were studied with cyclic voltammograms (CV), indicating that CV curves of the three PDIs were almost the same. The resulting values of E<sub>red, onset</sub>, E<sub>ox, onset</sub>, HOMO and LUMO were depicted

in Table S1. It is noted that the electrochemical band gap (HOMO-LUMO) was found to be similar for the three PDIs, while the HOMO (or LUMO) value for 4T-PDI was lower than that of 2T<sub>3</sub>-PDI and 4T<sub>3</sub>-PDI.

## 6. Electrochemical Synthesis and Characterization of the Polymer Films

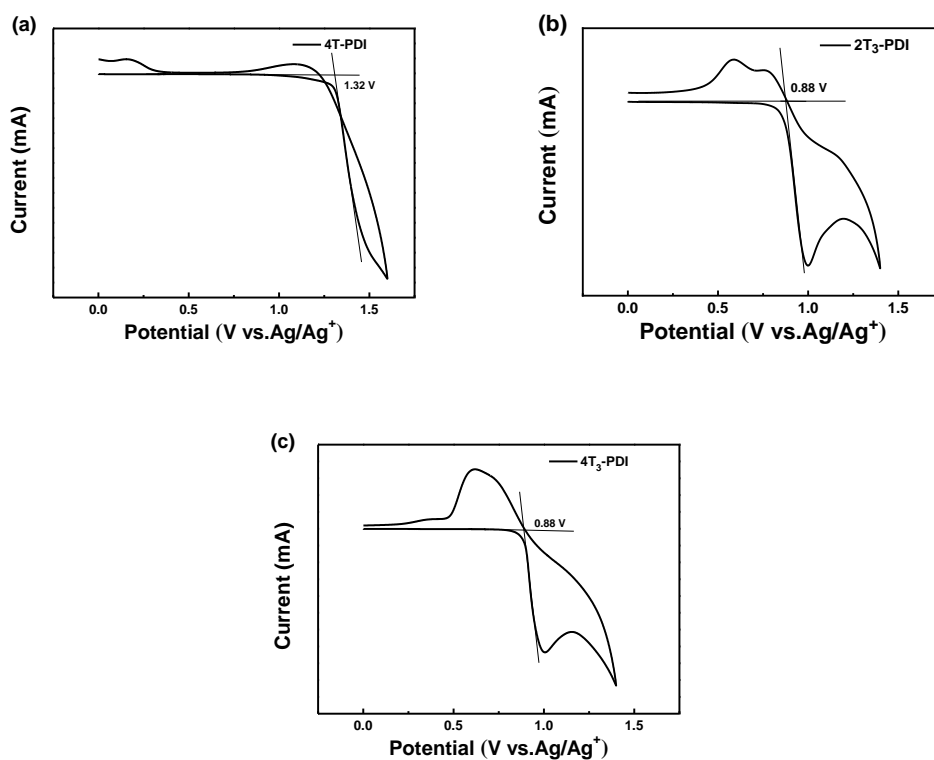


Figure S4. The first cycle of CV of the monomer molecules (0.015 mol L<sup>-1</sup>) recorded using ITO as the working electrode, Bu<sub>4</sub>NPF<sub>6</sub> as supporting electrolyte, (a) 4T-PDI, (b) 2T<sub>3</sub>-PDI and (c) 4T<sub>3</sub>-PDI. (scan rate of 100 mV s<sup>-1</sup>).

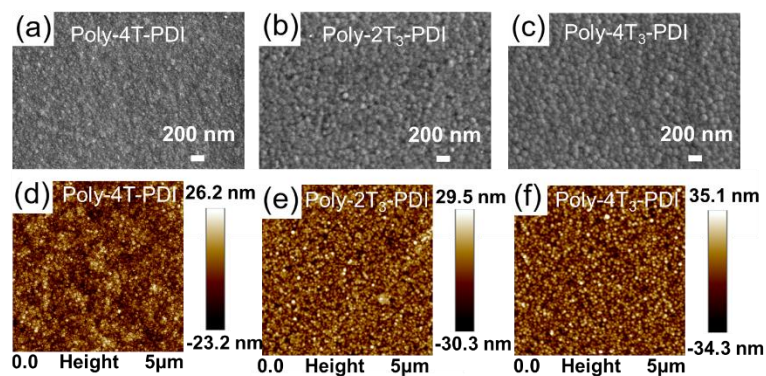


Figure S5. Morphology characterization of the three films deposited on the ITO electrode. SEM images: (a) poly-4T-PDI, (b) poly-2T<sub>3</sub>-PDI and (c) poly-4T<sub>3</sub>-PDI; AFM height images: (d) poly-4T-PDI, (e) poly-2T<sub>3</sub>-PDI and (f) poly-4T<sub>3</sub>-PDI.

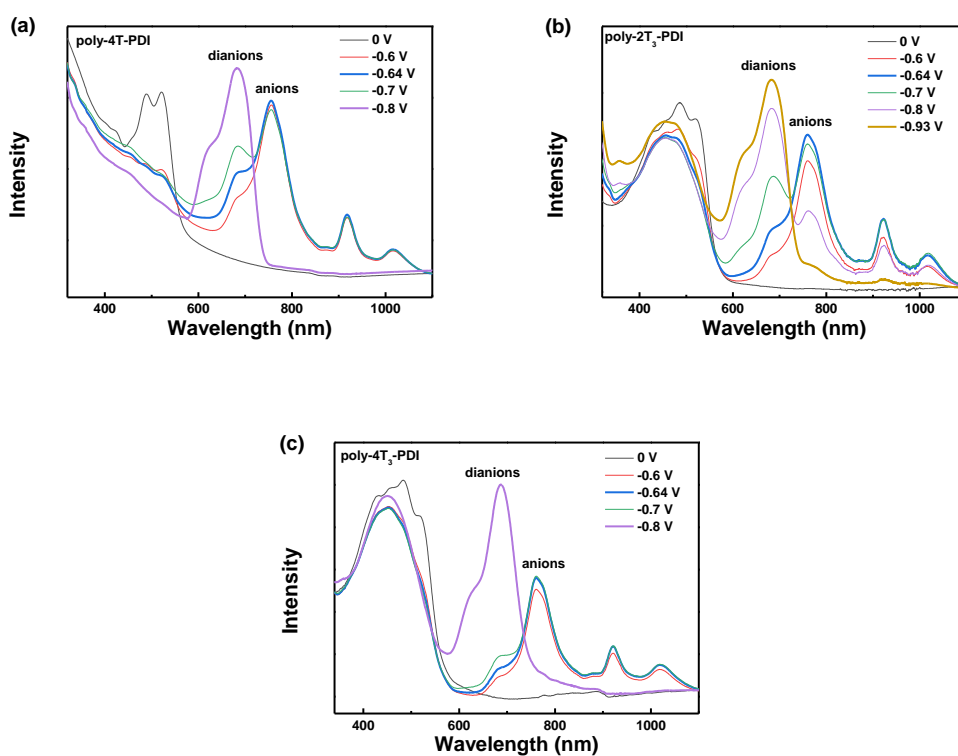


Figure S6. Spectroelectrochemical spectra of the polymer films in CH<sub>3</sub>CN containing 0.1 MBu<sub>4</sub>NPF<sub>6</sub> at different applied potentials (vs. Ag/Ag<sup>+</sup>).

We applied negative potentials to the three cross-linked polymer films for n-doping, and the spectroelectrochemical spectra were shown in Figure S6. When the applied

potential was decreased to -0.6 V, there were three new absorption peaks in the near infrared spectral region with the appearance of absorption maxima at 760 nm, 920 nm and 1020 nm, indicating the formation of PDI radical anions.<sup>4</sup> Further, when the applied potential was decreased to -0.8 V, the new absorption band with a maximum at 680 nm appeared and the absorption at 760 nm, 920 nm and 1020 nm disappeared. This transformation corresponds to the generation of PDI dianions.

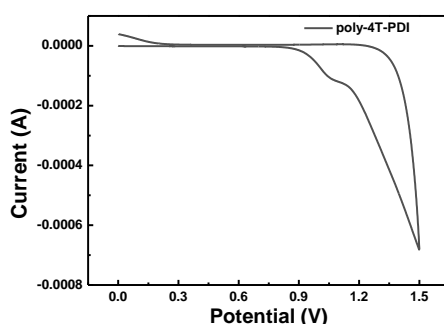


Figure S7. Cyclic voltammetry curves of the poly-4T-PDI film in the monomer-free electrolyte (0.1 M Bu<sub>4</sub>NPF<sub>6</sub> in acetonitrile), at a scan rate of 100 mV s<sup>-1</sup>.

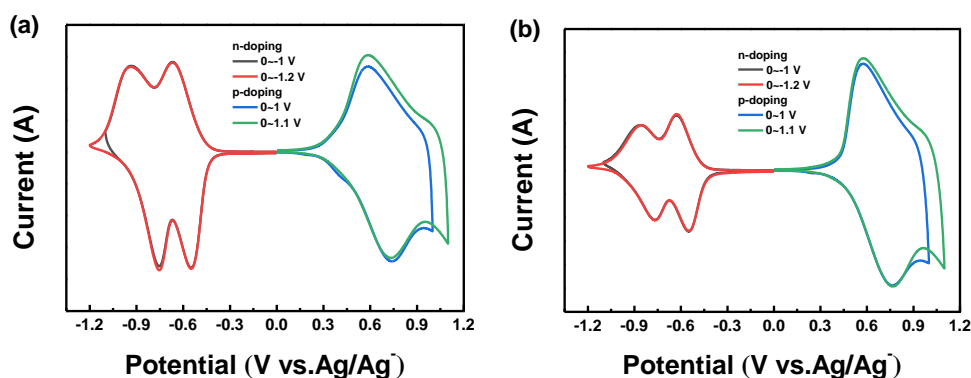


Figure S8. Cyclic voltammetry curves of the two cross-linked polymer films in the monomer-free electrolyte (0.1 M Bu<sub>4</sub>NPF<sub>6</sub> in acetonitrile), at a scan rate of 100 mV s<sup>-1</sup>.  
<sup>1</sup>. (a) poly-2T<sub>3</sub>-PDI, (b) poly-4T<sub>3</sub>-PDI.



Table S2. Electrochemical properties of poly-2T<sub>3</sub>-PDI and poly-4T<sub>3</sub>-PDI calculated from CV measurements. The values of Q<sub>p</sub> and Q<sub>n</sub> are obtained at the switching potential ranges given in Figure S8.

polymers	Q <sub>p1</sub> (10 <sup>-3</sup> C)	Q <sub>p2</sub> (10 <sup>-3</sup> C)	Q <sub>n1</sub> (10 <sup>-3</sup> C)	Q <sub>n2</sub> (10 <sup>-3</sup> C)	Q <sub>p1</sub> /Q <sub>n1</sub>	Q <sub>p1</sub> /Q <sub>n2</sub>	Q <sub>p2</sub> /Q <sub>n1</sub>	Q <sub>p2</sub> /Q <sub>n2</sub>
Poly-2T <sub>3</sub> -PDI	2.63	3.02	2.6	2.66	1.01	0.98	1.16	1.14
Poly-4T <sub>3</sub> -PDI	3.52	4.17	1.79	1.8	1.97	1.96	2.33	2.32

When applying negative potential from -1.1 to 0 V and -1.2 to 0 V, the absolute values of electric quantity as Q<sub>n1</sub> and Q<sub>n2</sub> were obtained by integrating the electricity consumption during the n-doping processes, respectively. When applying positive potential from 0 to 1 V and 0 to 1.1 V, the absolute values of electric quantity as Q<sub>p1</sub> and Q<sub>p2</sub> were obtained by integrating the electricity consumption during the p-doping processes, respectively. The Q<sub>p1</sub>, Q<sub>p2</sub>, Q<sub>n1</sub>, Q<sub>n2</sub>, Q<sub>p1</sub>/Q<sub>n1</sub>, Q<sub>p1</sub>/Q<sub>n2</sub>, Q<sub>p2</sub>/Q<sub>n1</sub> and Q<sub>p2</sub>/Q<sub>n2</sub> values are given in Table 1. Since poly-4T-PDI film is difficult to be p-doped, so we won't discuss it here. As shown in [Figure S8](#) and [Table S2](#), even if the different anodic and cathodic switching potentials were applied, the values of the anodic to cathodic doping charge ratio (Q<sub>p</sub>/Q<sub>n</sub>) for poly-2T<sub>3</sub>-PDI are closer to 1 than that of poly-4T<sub>3</sub>-PDI. This indicated that poly-2T<sub>3</sub>-PDI possesses more balanced n-doping and p-doping processes, which is highly beneficial to be used as ambipolar electrode materials.

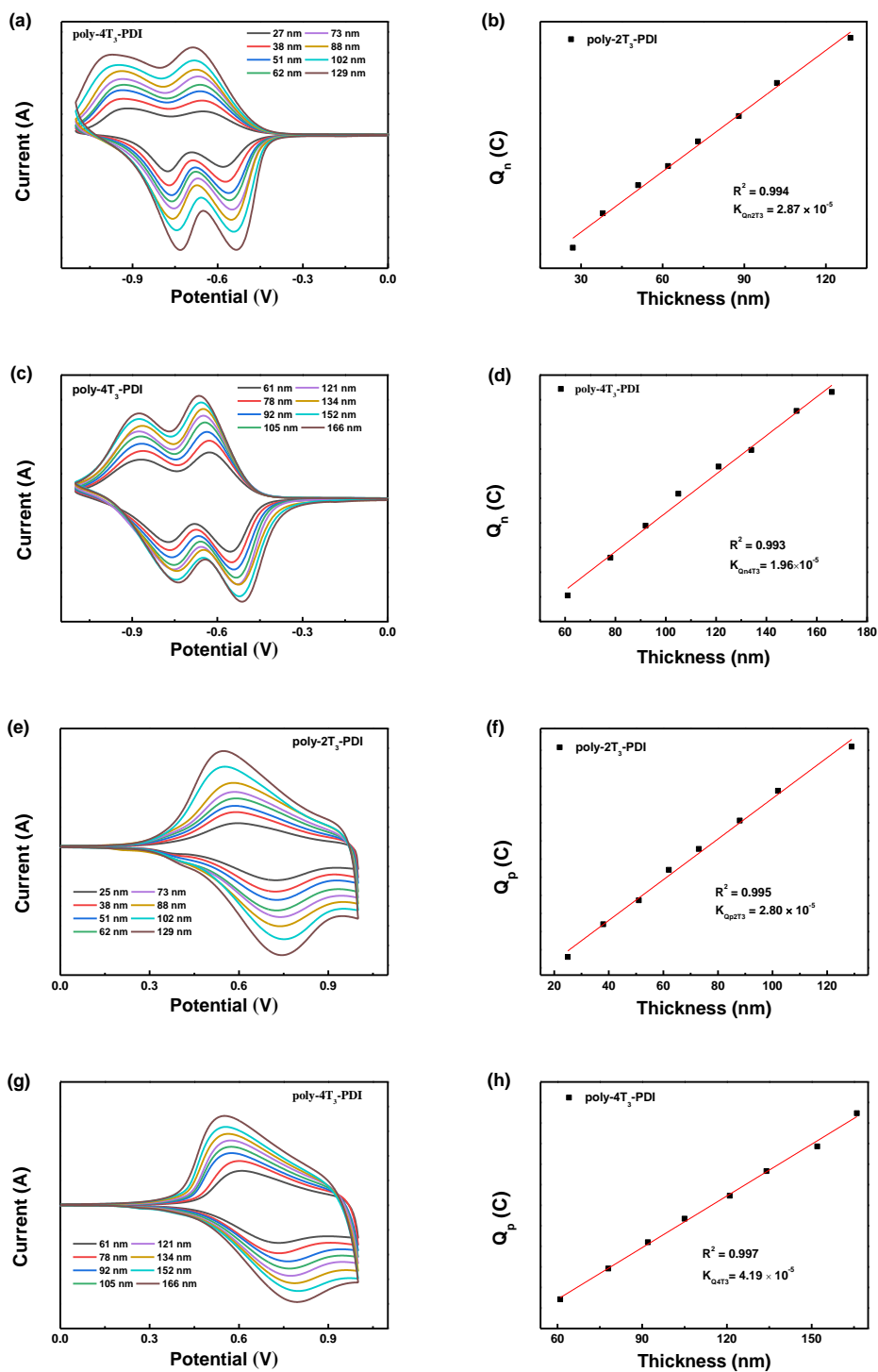


Figure S9. Anodic ( $Q_p$ ) and cathodic doping charge ( $Q_n$ ) at different films thickness.

For n-doping process, (a) and (b) poly-2T<sub>3</sub>-PDI, (c) and (d) poly-4T<sub>3</sub>-PDI; for p-doping process, (e) and (f) poly-2T<sub>3</sub>-PDI, (g) and (h) poly-4T<sub>3</sub>-PDI.

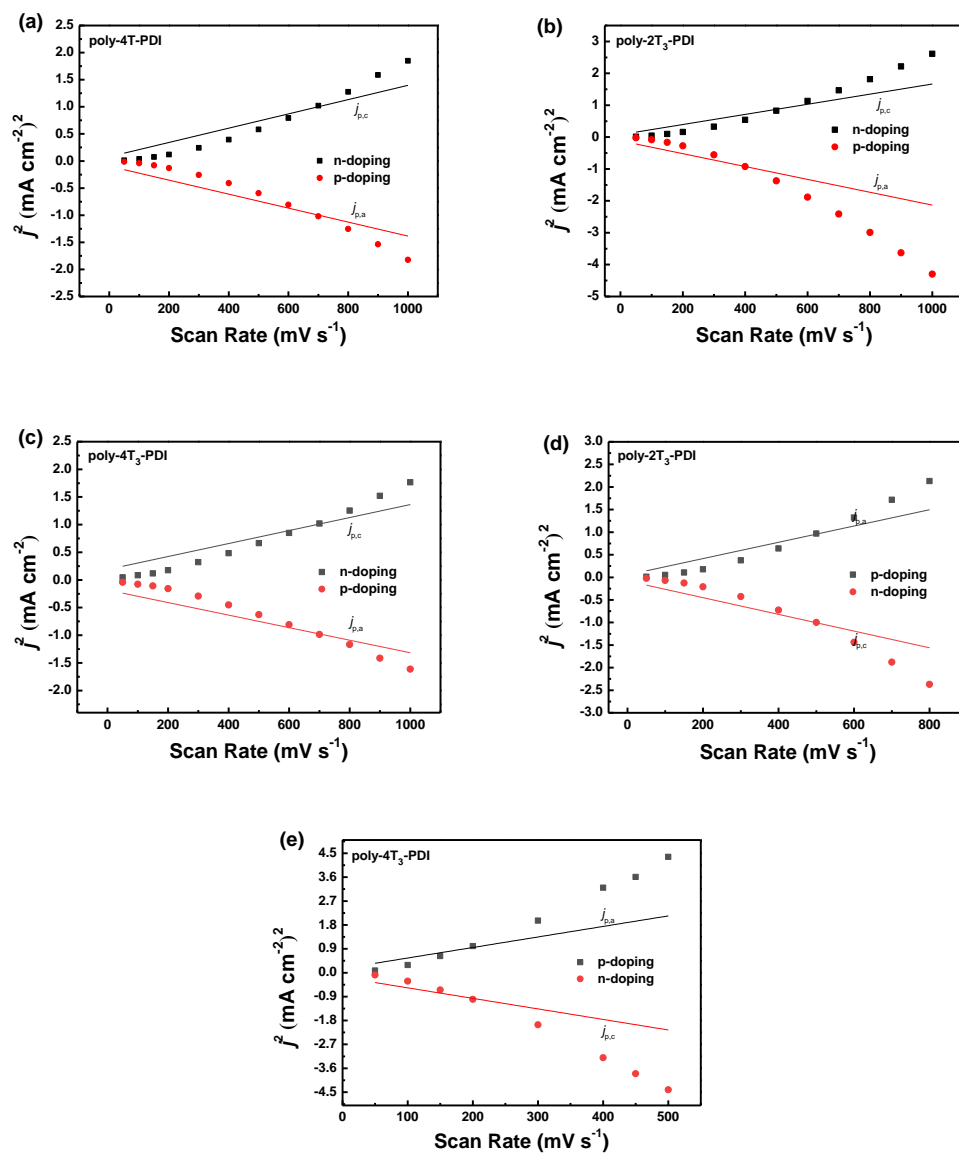


Figure S10. Relationship between CV peak currents and scan rates. (a) poly-4T-PDI, (b) poly-2T<sub>3</sub>-PDI and (c) poly-4T<sub>3</sub>-PDI for the n-doping process; (d) poly-2T<sub>3</sub>-PDI and (e) poly-4T<sub>3</sub>-PDI for the p-doping process.

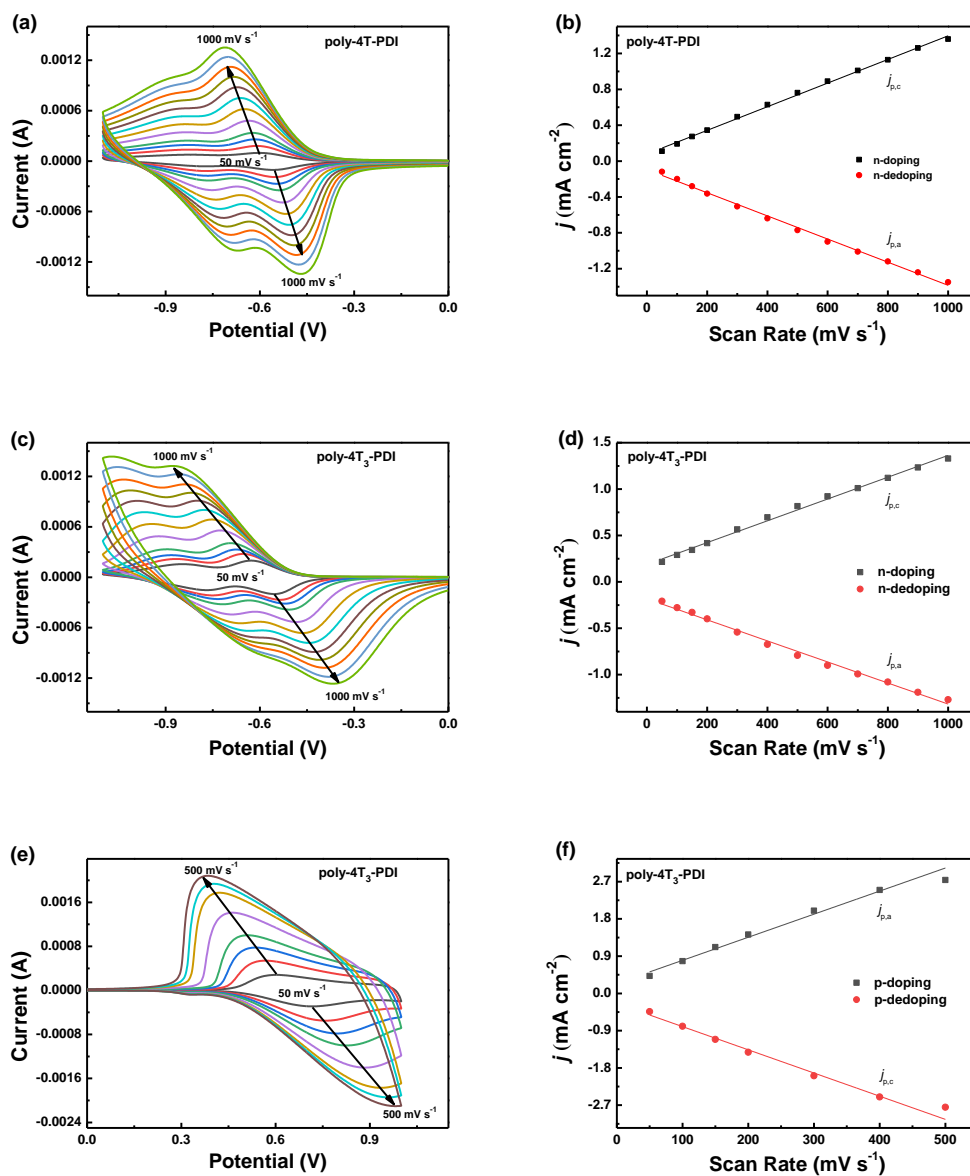


Figure S11. Cyclic voltammograms recorded at different scan rates. (a) poly-4T-PDI and (c) poly-4T<sub>3</sub>-PDI for the n-doping process; (e) poly-4T<sub>3</sub>-PDI for the p-doping process. (b, d, f) Relationship between CV peak currents and scan rates for the corresponding n-/p-doping processes.

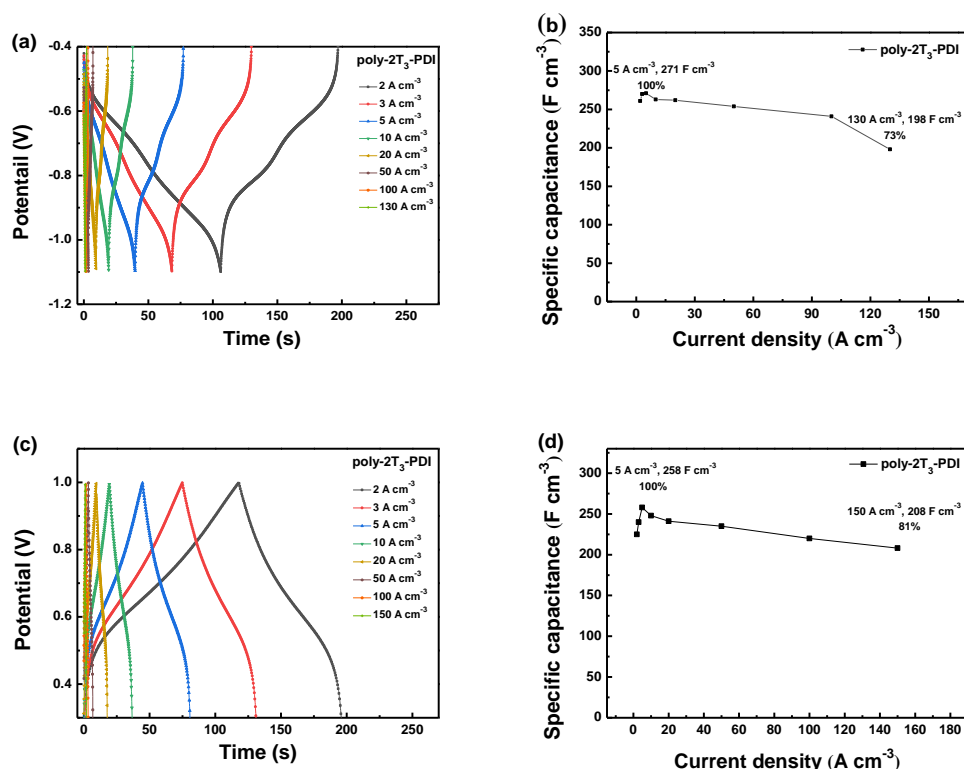


Figure S12. (a) Galvanostatic charge-discharge curves and (b) the volumetric capacitance of the poly-2T<sub>3</sub>-PDI film at different current densities between -0.4 V and -1.1 V. (c) Galvanostatic charge-discharge curves and (d) the volumetric capacitance of the poly-2T<sub>3</sub>-PDI film at different current densities between 0.3 V and 1 V.

For n-doping process, the measured volumetric capacitance value from the GCD curves of poly-2T<sub>3</sub>-PDI film was 271 F cm<sup>-3</sup> at the current density of 5 A cm<sup>-3</sup> (Figure S12a, b). Notably, even at an ultrahigh current density of 130 A cm<sup>-3</sup>, the capacitance of the film remains 76% of its highest value, revealing its outstanding high-rate stability. For n-doping process, the measured volumetric capacitance value from the GCD curves of poly-2T<sub>3</sub>-PDI film was 258 F cm<sup>-3</sup> at the current density of 5 A cm<sup>-3</sup> (Figure S12c, d). Notably, even at an ultrahigh current density of 150 A cm<sup>-3</sup>, the capacitance of the film remains 81% of its highest value, revealing its outstanding high rate stability.

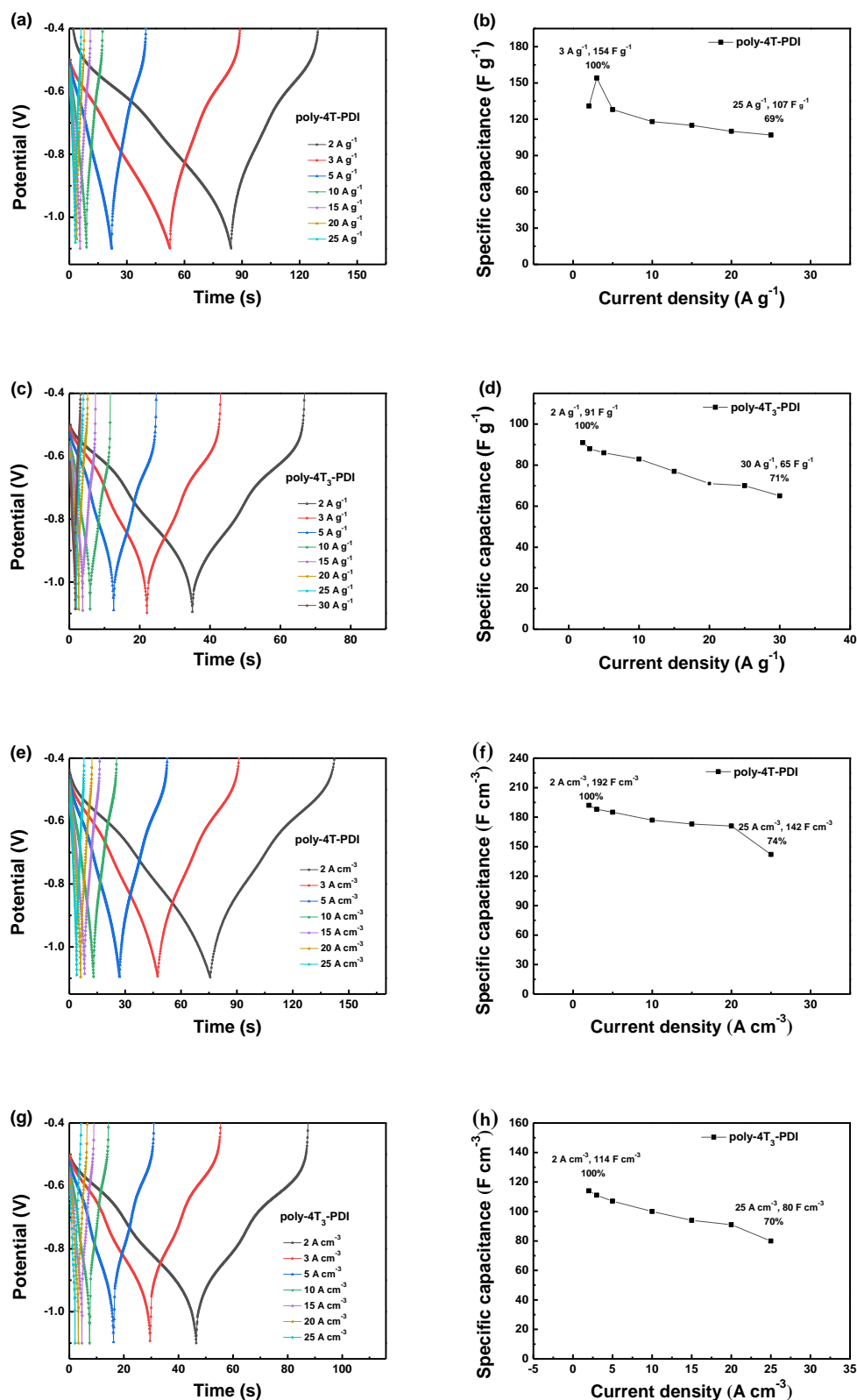


Figure S13. Galvanostatic charge-discharge curves of poly-4T-PDI and poly-4T<sub>3</sub>-PDI films at different current densities between -0.4 and -1.1 V (left) and the corresponding

specific capacitances and gravimetric capacitances of the two polymer films at different current densities, as indicated in Figures by legend.

For n-doping process, as shown in Figure S13, the specific capacitance of the poly-4T-PDI and poly-4T<sub>3</sub>-PDI film can be calculated from the GCD curves at different current densities. The gravimetric capacitance value of poly-4T-PDI film was 154 F g<sup>-1</sup> at the current density of 3 A g<sup>-1</sup> (Figure S13a, b). At a current density of 25 A g<sup>-1</sup>, the capacitance of the film remains 67% of its initial capacitance. The volumetric capacitance from the GCD curves, shown in Figure S13e, f, of the poly-4T-PDI film ranges from 192-142 F cm<sup>-3</sup> (at current densities from 2-25 A cm<sup>-3</sup>, respectively). The gravimetric capacitance value poly-4T<sub>3</sub>-PDI film was 91 F g<sup>-1</sup> at the current density of 2 A g<sup>-1</sup> (Figure S13c, d). At a current density of 30 A g<sup>-1</sup>, the capacitance of the film remains 69% of its initial capacitance. The volumetric capacitance from the GCD curves, shown in Figure S13g, h, of the poly-4T-PDI film ranges from 114-80 F cm<sup>-3</sup> (at current densities from 2-25 A cm<sup>-3</sup>, respectively). As a result, the specific capacitance of poly-4T-PDI and poly-4T<sub>3</sub>-PDI films were low, and moreover, it decreased rapidly with the increasement of current density, suggesting the poor charging/discharging rate stability of these two network films.

For p-doping process, as shown in Figure S14, the specific capacitance of the poly-4T<sub>3</sub>-PDI film can be calculated from the GCD curves at different current densities. The gravimetric capacitance value of poly-4T-PDI film was 234 F g<sup>-1</sup> at the current density of 3 A g<sup>-1</sup> (Figure S14a, b). At a current density of 25 g<sup>-1</sup>, the gravimetric capacitance of the film remains 71% of its initial capacitance. The volumetric capacitance from the

GCD curves, shown in Figure S14c, d, of the poly-4T-PDI film ranges from 211-162 F cm<sup>-3</sup> (at current densities from 2-25 A cm<sup>-3</sup>, respectively). As a result, the specific capacitance decreased rapidly with the increasement of current density, suggesting the poor charging/discharging rate stability of the polymer films.

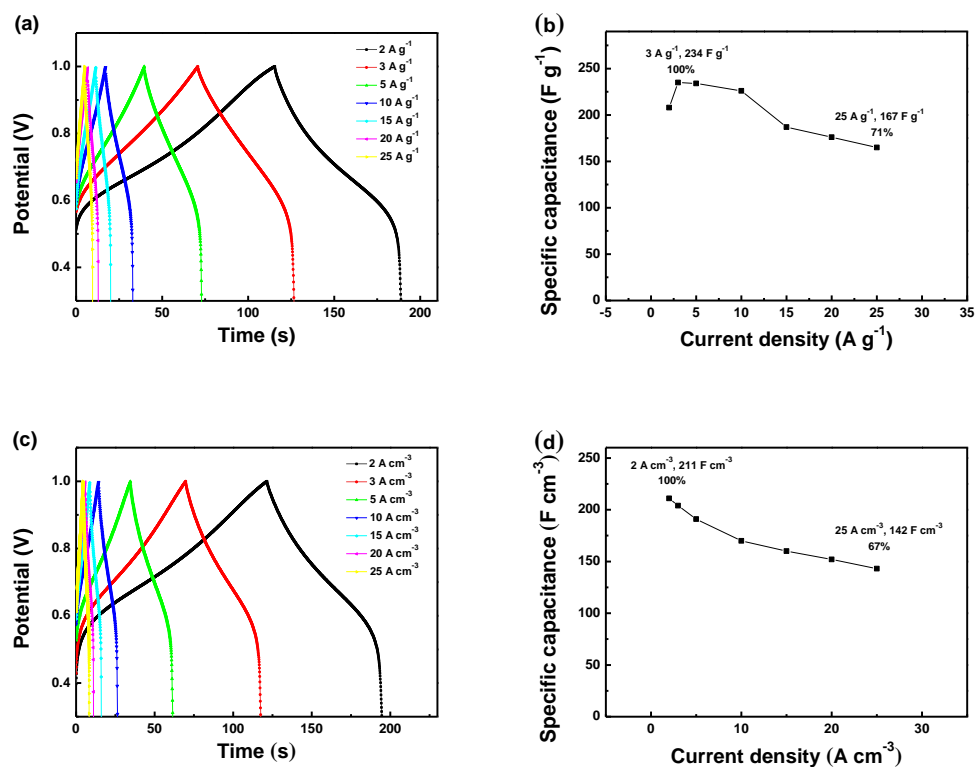


Figure S14. (a, c) Galvanostatic charge-discharge curves of poly-4T<sub>3</sub>-PDI at different current densities between 0.3 and 1.0 V. The specific (b) gravimetric and (d) volumetric capacitances of poly-4T<sub>3</sub>-PDI film at different current densities.



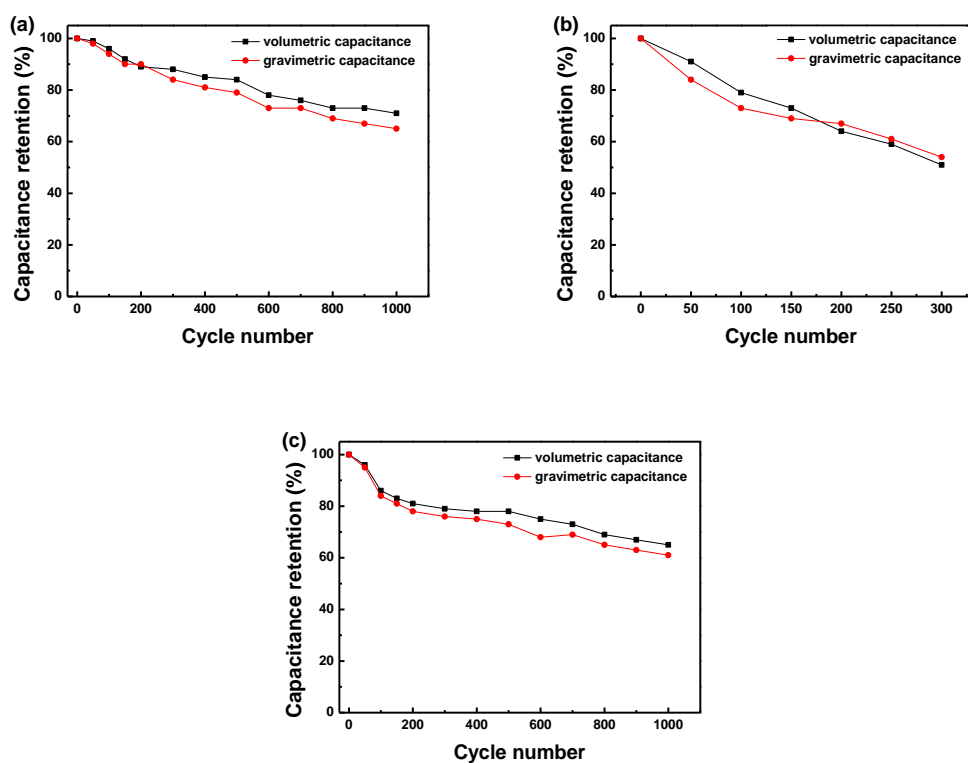
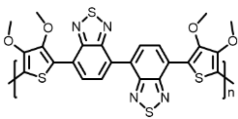
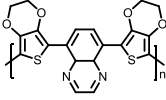
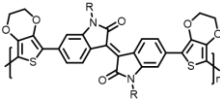
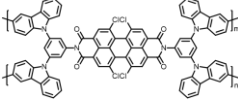
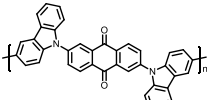
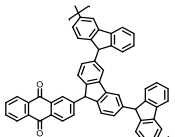
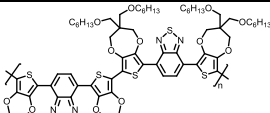
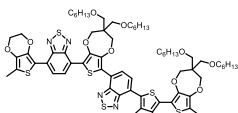
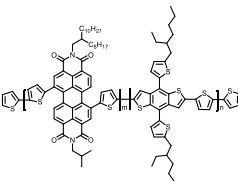


Figure S15. Cycle charge/discharge performance of poly-2T<sub>3</sub>-PDI film. (a) current density of 5 A g<sup>-1</sup> and 5 A cm<sup>-3</sup> and (c) current density of 120 A g<sup>-1</sup> and 120 A cm<sup>-3</sup> for the n-doping process, (b) current density of 5 A g<sup>-1</sup> and 5 A cm<sup>-3</sup> for the p-doping process.

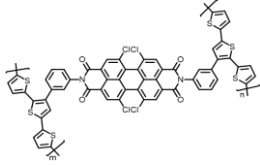
## 7. Capacitance of poly-2T<sub>3</sub>-PDI with literature

Table S3. Capacitance and stability of representative ambipolar polymer electrode materials reported in the literature.

Polymer structure	Electrode formation	Capacitance (condition and voltage range)
	Electrochemical deposition	Symmetric devices:
		72 F g <sup>-1</sup> , 0.5 A g <sup>-1</sup> (0.3 V) 91 F g <sup>-1</sup> , 50 mV s <sup>-1</sup> (2.5 V)
Ref. 5		

 <p>Ref. 5</p>	Electrochemical deposition	Symmetric devices: 40 F g <sup>-1</sup> , 0.5 A g <sup>-1</sup> (0.675 V) 201 F g <sup>-1</sup> , 100 mV s <sup>-1</sup> (2.5 V)
 <p>Ref. 6</p>	Electrochemical deposition	Single electrode: C <sub>mp</sub> : 1.7 mF cm <sup>-2</sup> (0.7 V) C <sub>mn</sub> : --- Device: 14 F g <sup>-1</sup> , 50 mV s <sup>-1</sup> (0.5 V)
 <p>Ref. 7</p>	Electrochemical deposition	C <sub>mp</sub> : 210 F g <sup>-1</sup> , 1 A g <sup>-1</sup> (0.7 V) C <sub>mn</sub> : 241 F g <sup>-1</sup> , 0.5 A g <sup>-1</sup> (0.7 V)
 <p>Ref. 8</p>	Electrochemical deposition	C <sub>mp</sub> : 473 F g <sup>-1</sup> , 50 mV s <sup>-1</sup> (0.34 V) C <sub>mn</sub> : 336 F g <sup>-1</sup> , 50 mV s <sup>-1</sup> (0.44 V) C <sub>all</sub> : 135 F g <sup>-1</sup> , 50 mV s <sup>-1</sup> (2.3 V)
 <p>Ref. 8</p>	Electrochemical deposition	C <sub>mp</sub> : 571 F g <sup>-1</sup> , 50 mV s <sup>-1</sup> (0.33 V) C <sub>mn</sub> : 286 F g <sup>-1</sup> , 50 mV s <sup>-1</sup> (0.32 V) C <sub>all</sub> : 133 F g <sup>-1</sup> , 50 mV s <sup>-1</sup> (2.1 V)
 <p>Ref. 9</p>	Spray coating	C <sub>mp</sub> : 156.8 F g <sup>-1</sup> , 0.05 mA cm <sup>-2</sup> (1.3 V) C <sub>mn</sub> : 107.4 F g <sup>-1</sup> , 0.05 mA cm <sup>-2</sup> (1.3 V) C <sub>all</sub> : 132.1 F g <sup>-1</sup> , 0.05 mA cm <sup>-2</sup> (2.6 V)
 <p>Ref. 9</p>	Spray coating	C <sub>mp</sub> : 135.9 F g <sup>-1</sup> , 0.05 mA cm <sup>-2</sup> (1.3 V) C <sub>mn</sub> : 106.6 F g <sup>-1</sup> , 0.05 mA cm <sup>-2</sup> (1.3 V) C <sub>all</sub> : 121.3 F g <sup>-1</sup> , 0.05 mA cm <sup>-2</sup> (2.6 V)
 <p>Ref. 10</p>	Spray coating	Single electrode: C <sub>all</sub> : 113 F g <sup>-1</sup> , 0.5 A g <sup>-1</sup> (~2.2 V) device: 42 F g <sup>-1</sup> , 0.5 A g <sup>-1</sup> (2.5 V)

---

	Electrochemical deposition	$C_{mp}$ : 264 F g <sup>-1</sup> , 5 A g <sup>-1</sup> (0.7 V) $C_{mn}$ : 299 F g <sup>-1</sup> , 5 A g <sup>-1</sup> (0.7 V)
This work		

---

## 8. Reference

- (1) Sharma, S.; Soni, R.; Kurungot, S.; Asha, S. K., Rylene Diimide-Based Alternate and Random Copolymers for Flexible Supercapacitor Electrode Materials with Exceptional Stability and High-Power Density. *J. Phys. Chem. C* **2019**, *123*, 2084-2093.
- (2) Wen, W.; Wu, J.-M.; Wang, Y.-D., Gas-sensing property of a nitrogen-doped zinc oxide fabricated by combustion synthesis. *Sensor. Actuat. B: Chem.* **2013**, *184*, 78-84.
- (3) Vasimalla, S.; Senanayak, S. P.; Sharma, M.; Narayan, K. S.; Iyer, P. K., Improved Performance of Solution-Processed n-Type Organic Field-Effect Transistors by Regulating the Intermolecular Interactions and Crystalline Domains on Macroscopic Scale. *Chem. Mater.* **2014**, *26*, 4030-4037.
- (4) Ma, W.; Qin, L.; Gao, Y.; Zhang, W.; Xie, Z.; Yang, B.; Liu, L.; Ma, Y. A perylene Bisimide Network for High-Performance n-Type Electrochromism. *Chem. Commun.* **2016**, *52*, 13600-13603.
- (5) DiCarmine, P. M.; Schon, T. B.; McCormick, T. M.; Klein, P. P.; Seferos, D. S. Donor-Acceptor Polymers for Electrochemical Supercapacitors: Synthesis, Testing, and Theory. *J. Phys. Chem. C* **2014**, *118*, 8295-8307.
- (6) Estrada, L. A.; Liu, D. Y.; Salazar, D. H.; Dyer, A. L.; Reynolds, J. R. Poly[Bis-EDOT-Isoindigo]: An Electroactive Polymer Applied to Electrochemical

Supercapacitors. *Macromolecules* **2012**, *45*, 8211-8220.

(7) Qin, L.; Ma, W.; Hanif, M.; Jiang, J.; Xie, Z.; Ma, Y. Donor-Node-Acceptor Polymer with Excellent n-Doped State for High-Performance Ambipolar Flexible Supercapacitors. *Macromolecules* **2017**, *50*, 3565-3572.

(8) Zhang, H.; Yao, M.; Wei, J.; Zhang, Y.; Zhang, S.; Gao, Y.; Li, J.; Lu, P.; Yang, B.; Ma, Y. Stable p/n-Dopable Conducting Redox Polymers for High-Voltage Pseudocapacitor Electrode Materials: Structure-Performance Relationship and Detailed Investigation into Charge-Trapping Effect. *Adv. Energy Mater.* **2017**, *7*, 1701063.

(9) Wang, Y.; Li, W.; Guo, Y.; Cao, J.; Murtaza, I.; Shuja, A.; He, Y.; Meng, H. Recombination Strategy for Processable Ambipolar Electroactive Polymers in Pseudocapacitors. *Macromolecules* **2018**, *51*, 7350-7359.

(10) Sharma, S.; Soni, R.; Kurungot, S.; Asha, S. K. Rylene Diimide-Based Alternate and Random Copolymers for Flexible Supercapacitor Electrode Materials with Exceptional Stability and High Power Density. *J. Phys. Chem. C* **2019**, *123*, 2084-2093.